MR Artifacts: A Review

Errol M. Bellon[1-3]
E. Mark Haacke[1, 4]
Paul E. Coleman[3]
Damon C. Sacco[1, 2]
David A. Steiger[1, 2]
Raymond E. Gangarosa[3]

The process of creating MR images frequently gives rise to artifacts in the final display. Many artifacts may be corrected or ameliorated through an understanding of their cause. This requires familiarity with scanner design; theory of operation; and image acquisition, generation, and display. Some artifacts are obvious, totally degrading the image; others are regional, leaving much of the scan undisturbed. In some cases, the degradation is permanent; in others, the data can be reprocessed or manipulated to yield artifact-free images. Some artifacts are overt and easily identified. Others, such as those caused by phase-shift or gradient-strength effects, are subtle and require careful observation for detection.

The acceptance of MR imaging in clinical practice has brought with it a requirement for recognition and understanding of the various artifacts that may occur during each step of the scanning process, from data acquisition through image display. As is the case with each of the other radiologic techniques, numerous artifacts are associated with MR scanning [1–5]. With an understanding of their cause, many may be corrected, minimized, or avoided, either at the source before data acquisition or at the reconstruction stage after data acquisition. Although artifacts are capable of causing severe image degradation, many more subtle effects exist that can also lead to misinterpretation of the image. Our main concern here is to draw attention to both the subtle and obvious changes in contrast that may lead to misdiagnosis.

Artifacts are a problem in MR imaging because the complexity of the imaging sequences introduces the opportunity for multiple sources of systematic error. Physical constraints, such as the presence of field inhomogeneity, and hardware limitations contribute further problems. Also, numerous sources of spurious noise (both sequence- and system-related) can cause image degradation.

The various artifacts may conveniently be considered under the following headings: sequence, reconstruction algorithm, field, and noise. Each category can in turn be subdivided into system- and patient-related artifacts. Many of the artifacts demonstrated here were deliberately generated for illustrative purposes. They in no way represent the image quality to be expected from a properly functioning, well-calibrated scanner.

Technique and Methods

Two-dimensional Fourier transform (2DFT) imaging is now the standard method for acquiring data in MR imaging [6]. The most common technique is the spin-echo sequence (Fig. 1) used to refocus static field inhomogeneities. This sequence requires the application of a 90° RF pulse to rotate the magnetization into the plane transverse to the static magnetic field. A gradient is often applied in one direction during the RF to select a slice of interest. At an echo time (TE) of TE/2 later, a 180° refocusing RF pulse is applied so that at a time TE

Received February 14, 1986; accepted after revision June 27, 1986.

The work on which this report is based was carried out at the Clinical Science Center, NMR Division, Picker International, Highland Heights, OH (Surya Mohapatra, Director).

[1]Department of Radiology, Case Western Reserve University, Cleveland, OH 44106.

[2]Department of Radiology, Cuyahoga County Hospital, 3395 Scranton Rd., Cleveland, OH 44109. Address reprint requests to E. M. Bellon.

[3] Clinical Science Center, Picker International, Highland Heights, OH 44143.

[4]Department of Physics, Case Western Reserve University, Cleveland, OH 44106.

AJR 147:1271–1281, December 1986
0361–803X/86/1476–1271

after the initial excitation the magnetization refocuses or echoes even in the presence of field inhomogeneities. The data are then sampled centered about this time.

In order to extract two-dimensional information, the spins are spatially encoded in one direction by phase encoding and in the other by frequency encoding. This is accomplished in the latter case by applying a dephasing gradient between the 90° and 180° pulses and then a rephasing or read gradient centered about TE so that the spins still echo at TE. In the former case, the phase encoding can take place before or after the 180° RF pulse but must be changed each time the sequence is rerun. Each such collection of data is referred to as a view, with all views collectively representing a complete scan. The time between each view is the repetition time (TR).

The number of sample points and the number of views determine the amount of spatial information or resolution for that scan. The field of view (FOV) is also determined by the appropriate choice of sampling time and gradient strength. Smaller FOVs are normally achieved by increasing the gradient strength. Finally, the data are sampled and a two-dimensional discrete inverse Fourier transform performed to produce an image. Most images presented in this article are based on spin-echo sequences with the parameters: sampling time, 80 μsec; read gradient, 1 mT/m; FOV, 30 cm (head), 45 cm (body); sampling points, 256; and views, 256. Where deviations from this parameter set occur, the values of the modified parameters will be stated.

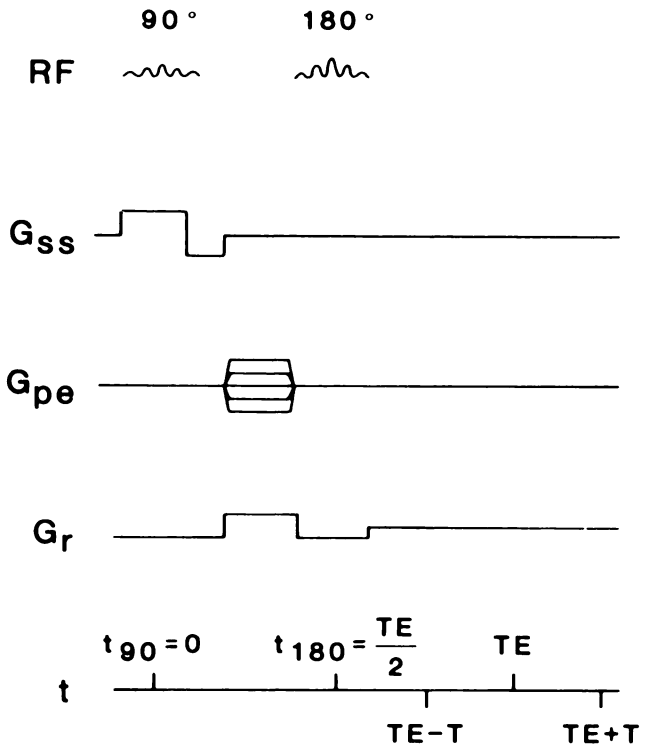

Fig. 1.—Standard 2DFT sequence structure showing radiofrequency and gradient timing and profiles. Timing (t) is counted from center of 90° pulse, with echo occurring at t = TE. Sampling runs from TE − T to TE + T being of duration T_s = 2T. G_{ss} = section select gradient; G_{pe} = phase encoding gradient; G_r = read gradient.

Sequence Artifacts

System-Related

Inherent in all MR techniques is the assumption that the RF pulses are ideal. For example, in a spin-echo multislice experiment, it is assumed that slices have square profiles and the RF field distribution is uniform throughout the plane. Deviations from ideal pulses can cause various artifacts: broad slice profiles or perfect thick slices produce partial-volume effects (Fig. 2A), and profiles with multiple lobes produce scan sections that contain contributions from out-of-slice material (Fig. 2B). In the former case, a small tumor could be lost in a thick slice if surrounded by high-intensity tissue. (However, even going to a thin slice may not allow identification of the tumor if contrast-to-noise is now too low.) The latter is caused by 180° pulses acting as 90° pulses

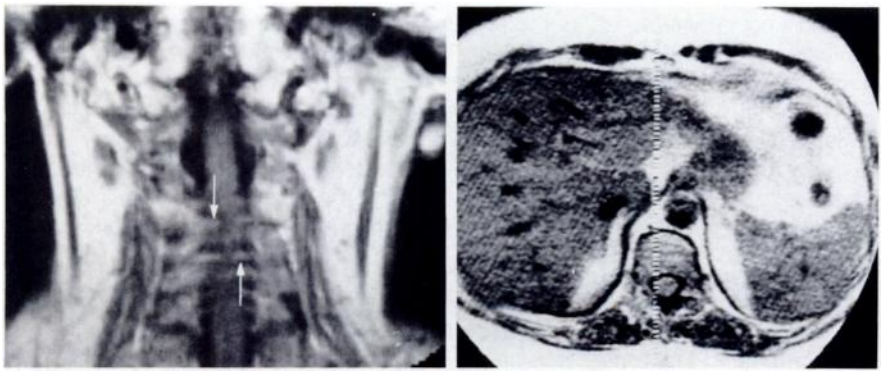

Fig. 2.—Partial-volume effect.
***A*, Coronal section through cervical spine at nominal 10-mm section thickness contains information from outside ideal slice. Note transverse contributions (*arrows*) from intervertebral disks anterior to plane of section, projecting faintly over cord (TR 700, TE 40).**
***B*, Out-of-slice contribution in region of liver, with single acquisition. Vertical line with alternating intensity colloquially referred to as the "zipper" artifact.**

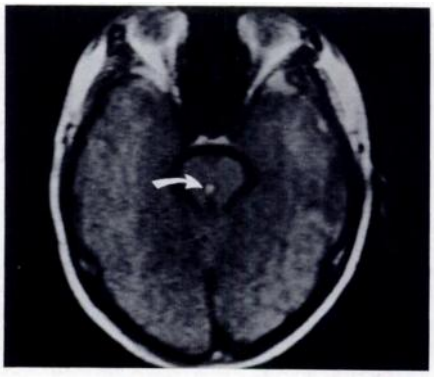

Fig. 3.—Central point artifact. When direct current level of each view in scan is not constant, line artifact occurs in phase-encoded direction. When all views have same direct current offset, line reduces to a point artifact (*arrow*). Image is a transverse pilot brain scan with 128 phase-encoding steps (views) and TR 200, TE 40.

outside the slice and is overcome by appropriately phase-alternating one of the pulses and combining the data from two acquisitions. This twofold excitation removes the artifact. When clinical requirements necessitate a short scan time and only a single acquisition is used, the resulting artifact is a line (or lines) through the image along (parallel to) the frequency-encoded axis. With ideal RF pulses, high-quality, artifact-free images are routinely obtained, even with one acquisition.

A similar artifact occurs if the direct current (DC) level of each phase-encoding step (view) in the scan is not constant. This leads to a line along the phase-encoded axis. If all views have the same DC offset, the artifact reduces to a central point (Fig. 3). This point actually gets spread over several pixels because of the finite number of data points used. It may be particularly troublesome if located over a clinically significant region. For example, when the artifact falls over the midbrain or pons, it needs to be distinguished from a small infarct. The solution again involves appropriate RF phase cycling and data subtraction.

Image quality is also sensitive to the read-gradient level. The read gradient and the size of the FOV together determine the sampling rate and hence the frequency content per pixel in the image. Normally, the read gradient is set high to minimize field inhomogeneity effects. However, if the ratio of total sampling time (T_o) to the T_2 value is on the order of unity, image contrast and resolution will change. Such may be the case with body scanning where this effect may be pronounced, especially with low read gradients (Fig. 4). This edge enhancement due to finite T_2 values should not be confused with the Gibbs phenomenon caused by data truncation (see discussion of patient-related noise artifacts).

A practical problem also associated with the gradients is the correct setting of the FOV. If the FOV selected is too small, the image will wrap back into itself (aliasing). Nevertheless, if the overlap does not obscure the region of interest, the image is still usable (Fig. 5). A FOV that produces aliasing may be a deliberate choice to obtain a higher-resolution image in a central region of interest. This aliasing may be avoided even with the incorrect setting in the frequency-encoded direction if the analog filter bandwidth is reduced accordingly. This is not possible in the phase-encoded direction because of the discrete steps used.

Patient-Related

Since the patient has electric and magnetic properties (such as conductivity, permitivity, and permeability) different from free space, it is not possible to have uniform distribution of

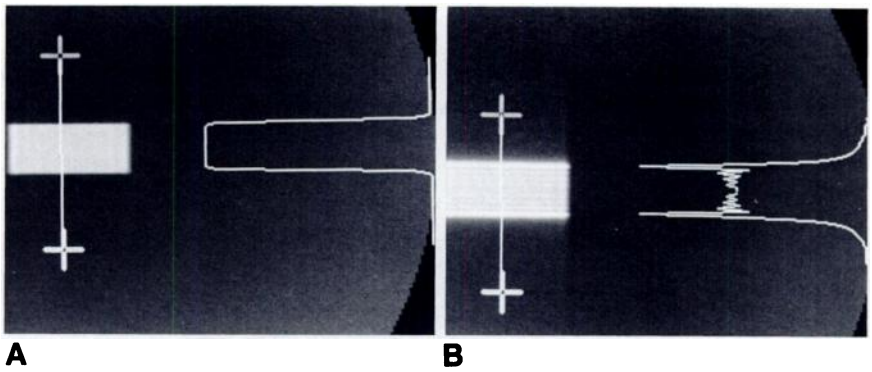

Fig. 4.—Read gradient and size of field of view together determine sampling rate and thus frequency content per pixel. Image contrast and resolution are affected by setting of read gradient, especially low read-gradient levels.

***A*, Simulated image of rectangular box with R = $T_o/2T_2$ = 0.03.**

***B*, As in *A*, but with R = 1.28. Note edge enhancement and increase in systematic noise in central region. There is also loss of resolution at edges due to increased dispersive nature of signal.**

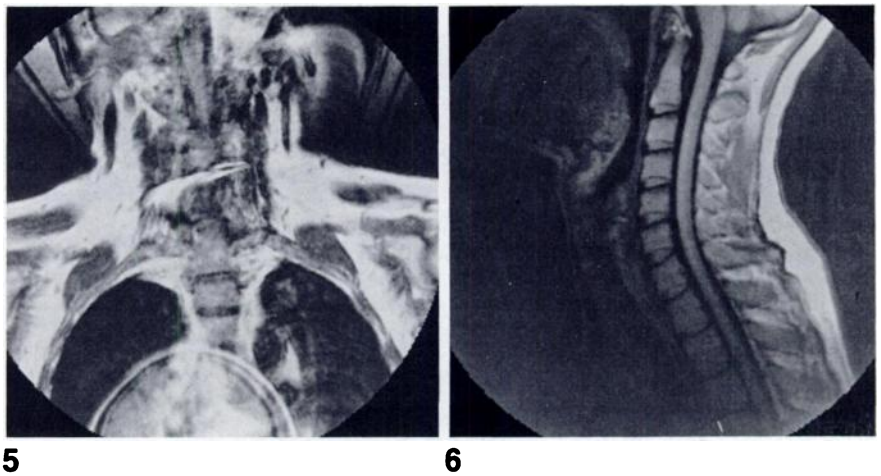

Fig. 5.—Aliasing—image appears wrapped around into itself. Picture elements that correctly belong at top of field are projected along bottom, and vice versa. Vertical phase-encoding was used for this scan; when horizontal phase-encoding is used, artifact occurs along left and right margins instead. Artifact occurs because field of view selected is too small for particular body region being imaged. Note that although artifact is usually present peripherally, central regions of image are unaffected and quite usable.

Fig. 6.—Surface-coil hot spot. Response of the particular coil employed here varies as function of position, so tissues close to coil are imaged much more intensely than those farther away. In this case, subcutaneous fat near coil is much more intense than farther away from coil. Note also lack of resolution in anterior neck structures. The problem is due to nonuniform reception of signal throughout scan slice.

an RF pulse throughout the scan slice [7]. This leads to an RF penetration problem where a tissue of uniform composition exhibits a change in intensity depending on its location in the image plane. Similar, but less complicated, effects occur when using surface coils [8] where their response varies as a function of position, thus producing intense regions close to the coil with significant falloff in tissue farther away from the coil (Fig. 6).

The signal from flowing blood can be significantly affected by the sequence parameters [9]. For example, flowing blood can appear hyper- or hypointense depending on the rate and direction of flow, whether the sequence used was single- or multislice, and whether broad-band or selective pulses were used. A knowledge of vascular anatomy is essential for the differentiation of low-intensity areas on T1-weighted images, so as to permit distinction of vascular structures from neoplasm or other abnormality. Flowing blood can also produce an artificially enhanced signal [10, 11], so that before pathologic conditions can be diagnosed, the possibility of artifactually enhanced areas caused by flowing blood should be excluded.

Reconstruction Algorithm Artifacts

System-Related

The mainstay of current sequence design and reconstruction algorithms is 2DFT imaging. The types of artifact associated with this method are different from those associated with other techniques (such as projection reconstruction, echo planar [12], and Hybrid [13, 14]). In this article, only 2DFT-related techniques will be considered.

The peak signal changes drastically as a function of sequence and object being imaged, so that the signal is attenuated to make the peak signal compatible with the computational range of the computer. If the signal does not lie within the required limits, data clipping occurs (the large numbers become smaller numbers lying in the available integer range) and information is destroyed and is not recoverable. In this case, the image is often rendered useless (Fig. 7), even though only a small central portion of the data is corrupted (see also Fig. 9).

Another example is hardware failure during the experiment, with only one data channel surviving. The image will appear as if it has been reflected about both the phase-encoded axis and the frequency-encoded axis [1] (Fig. 8). However, in those regions where no overlap occurs, the information is still accurate and diagnostically useful.

Patient-Related

The data-clipping artifact can also occur if there is patient movement during the period the signal attenuator is being set. For example, with respiratory motion, a bowel loop may move in and out of the plane of interest. Since bowel tissue has characteristics different from other tissues, including those in the plane of interest, setting the attenuator when a bowel loop is in the plane will produce an incorrect attenuator setting with respect to the desired plane. This may lead to data clipping for that plane if the attenuator setting is not determined for a sufficient length of time.

Flow and motion within the subject also lead to image degradation and changes in contrast. This is manifest by a

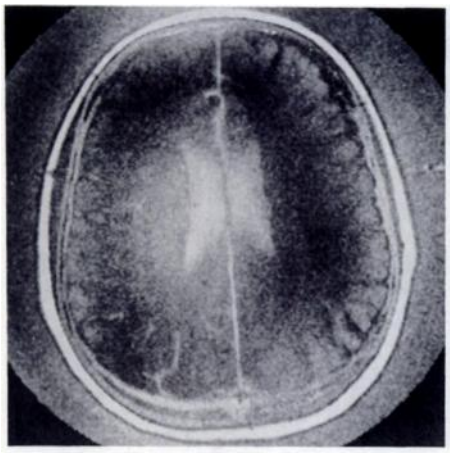

Fig. 7.—Data clipping. If peak signal does not lie within computational range of computer and software used in image reconstruction, severe arithmetic errors occur, and incorrect pixel values are assigned. Image has significant low spatial frequency distortion giving it a "ghostlike," unreal quality with loss of contrast and resolution.

Fig. 8.—Failure of one data channel, an example of hardware failure. Image resembles that caused by aliasing (Fig. 5), but is reflected about both phase-encoded and frequency-encoded axes. There are small regions where no overlap occurs and image is still usable (TR 600, TE 40).

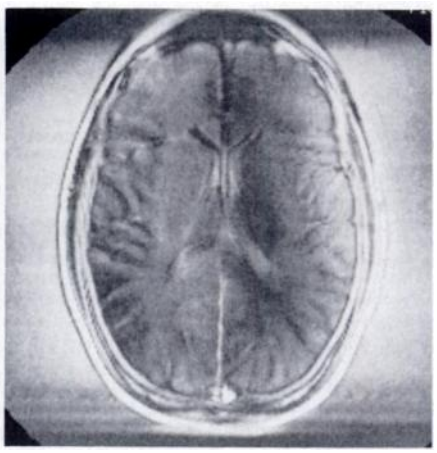

Fig. 9.—Motion during central view acquisition. Normal volunteer was instructed to turn the head to the side once only during a few central scan views (near view 128) and then resume original scan position. The scan had 256 phase-encoding steps (views). The image is totally degraded, shows altered contrast, and a "ghostlike" quality similar to data clipping (compare with Fig. 7). Movement early (near view 5) or late (near view 250) does not degrade image.

loss in resolution for motion and by phase-encoded noise through the affected region for both motion and flow. The simple 2DFT algorithm is not equipped to handle the phase errors associated with motion; however, an appropriate reconstruction technique may be able to do so [15]. The induced phase-encoded noise aspect of this problem and methods of alleviating the problem are addressed under Noise Artifacts. The use of phase-ordering techniques [14, 16] during data acquisition eliminates the noise in the phase-encoded direction, leaving only the resolution loss due to gross body-part motion itself. Scaling techniques [15, 17] operating on the raw data may then be used to further improve the resolution.

An image with loss of resolution only may also occur if the patient moves during the critical period when the central views (region of zero or low phase-encoding) are being acquired. Either a single deep inspiration or turning of the head is sufficient to produce severe image degradation (Fig. 9).

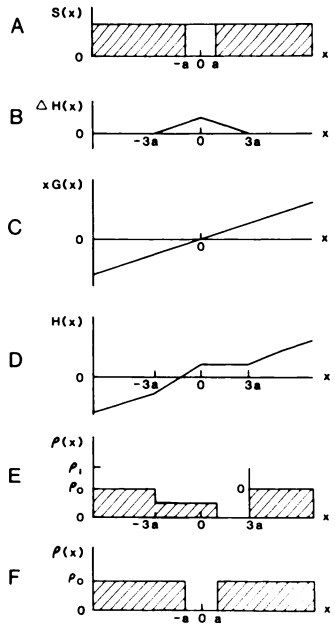

Fig. 10.—Geometric (field) distortion in frequency-encoded direction: effect of field inhomogeneity. Artifactual expansion or contraction, as well as intensity change and altered contrast and resolution, result from macroscopic imperfections in magnetic field, especially due to magnetic substances.

***A*, Cross section of hypothetical object. Cross-hatched area denotes normal tissue, and unmarked area contains material with significantly different susceptibility of length 2a.**

***B*, Hypothetical field inhomogeneity (true field profile has been simplified for purpose of illustration).**

***C*, Field due to applied gradient.**

***D*, Total field.**

***E*, Image intensity as function of position. Here $\rho_1 = \rho_0[1 + (\alpha/3\Delta\chi)]$, where $\Delta\chi$ is pixel size.**

***F*, Ideal image intensity.**

Field Artifacts

System-Related

The relationship between the read-gradient level and the FOV, which together determine the sampling rate and hence the frequency content per pixel in the image, was discussed under Sequence Artifacts. Particularly in the case of body scanning, and in situations where low read gradients are used, field inhomogeneity effects may result in altered image contrast and resolution.

Geometric distortion only occurs along the frequency-encoded axis and arises because macroscopic imperfections of the magnetic field lead to nonparallel flux lines that, when mapped onto an orthogonal (square) grid, cause deformation of the image. These imperfections may be caused by large static field inhomogeneities or by field changes resulting from the presence of a magnetic substance in an otherwise constant field. The induced field deviations produce artifactual expansion or contraction of the image, accompanied by changes in image intensity and resolution. For demonstration purposes (Fig. 10), let the substance induce a field change (G') linear to the center of the modified region and of opposite slope and equal magnitude beyond the center, as shown in Figure 10B. Taking the magnitude to be the same as that of the read gradient (G), one can easily see that in the region of the increased field gradient (Fig. 10D), the object appears stretched, decreasing the image intensity while simultaneously increasing resolution (Fig. 10E). Conversely, where the field is now constant, the object gets mapped to a point. Since this information has been collapsed to a point, the image intensity is increased and all resolution is lost. While ferromagnetic objects cause the field deformations discussed above, diamagnetic objects cause much smaller changes and the stretching and compressing are reversed with respect to the frequency direction.

The ratio G'/G determines the degree of stretching and compression. This can be expressed equivalently by the ratio $\gamma\Delta H/\Delta f$, where ΔH is the field inhomogeneity across a pixel and Δf ($= \gamma G\Delta\chi$) is the frequency per pixel. Since the size of the read gradient controls the amount of distortion, allowable changes in TE or TR will not affect the distortion. Unfortunately, although an increase in the read gradient will reduce the distortion, it will also decrease the signal to noise (S:N) ratio. This can be understood since, as the bandwidth increases by a factor of A, the incoherent (white) noise increases by a factor of $\sqrt{A}$. In some cases, suffering the slight distortions may well be worth the extra S:N margin.

The effect of the field distortions may be central or peripheral, symmetric or asymmetric, and the distortion produced may be pincushion- or barrel-type. While the clinical impact of the artifact is that linearity of the image is lost, resolution may actually be degraded or enhanced. As an example, vertebral bodies may appear smaller or larger at the periphery of the field than at the center (Fig. 11).

Patient-Related

As discussed above, ferromagnetic objects produce artifacts because their higher magnetic susceptibility relative to tissue produces localized field changes. This results in image distortion and associated contrast changes [18–20]. The direction of the misregistration is determined by the direction of the read gradient used for the particular MR experiment. As described earlier, the characteristic appearance on the image is a low-intensity region or void adjacent to or surrounded by regions of high signal intensity (Fig. 12). Very often bizarre, nonanatomic, elongated distortions are seen (Fig. 13). Depending on the quantity, shape, and susceptibility of the metal present, there may be so much distortion as to make the image anatomically unrecognizable.

While metals are classified as ferromagnetic and diamagnetic, the mechanism of image distortion is the same in both cases, differing only in magnitude and direction. A ferromag-

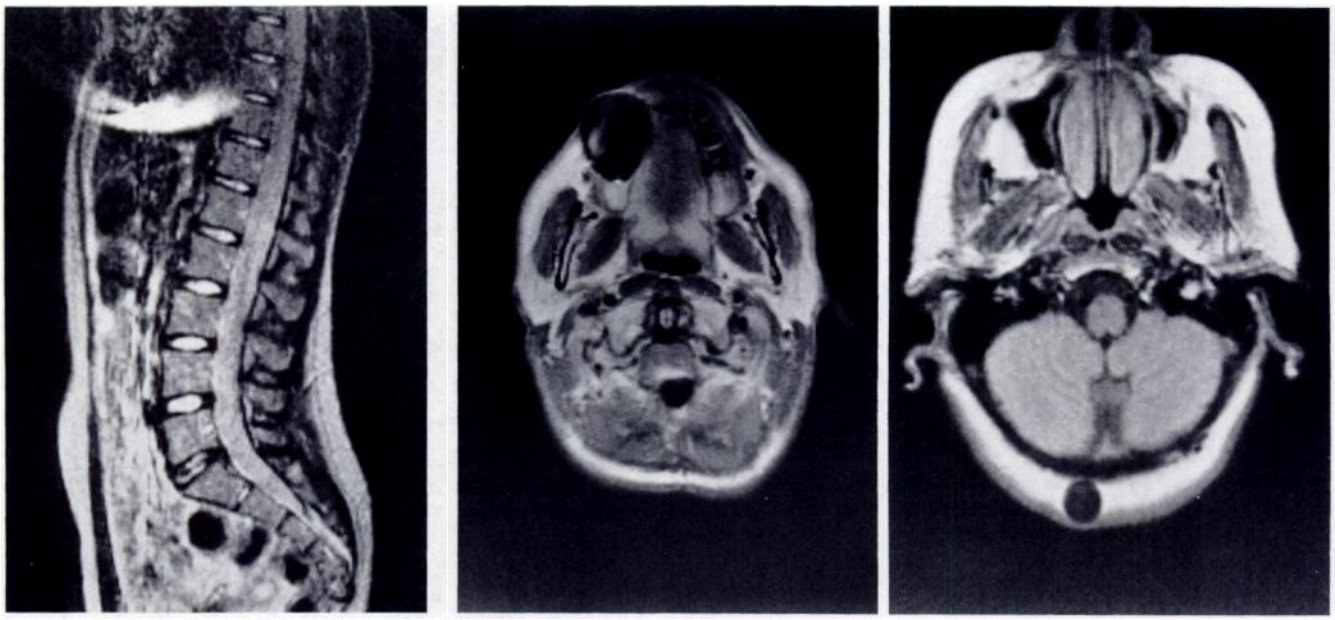

Fig. 11.—Field distortion—loss of linearity. Vertebral bodies appear disproportionately smaller at top and bottom of image than at center. Image is not linear. This may occur along one of or both x and y axes. Note that resolution may in fact be enhanced or degraded. (Aliasing artifact partially obscures upper portion of field.)

Fig. 12.—Typical ferromagnetic artifact. Low-intensity central region in *A* is partly surrounded by a high-intensity border along same direction as read gradient. This requires distinction from true pathologic abnormality, such as scalp fibroma in *B*, which exhibits low-intensity central region, but lacks peripheral zone of intensity.

netic surgical clip will produce a larger void area than an equivalently sized nonferromagnetic clip. Substances not thought to contain ferromagnetic materials, such as dental crowns, in fact frequently are not made of precious metals and may contain significant quantities of nickel, cobalt, or chromium, in which case they do produce severe artifacts. Dental amalgam contains silver, tin, and mercury (occasionally tin substitutes for the silver) and does not produce artifacts. Ferromagnetic material is present in wire surgical sutures, protheses of all kinds, zippers, safety pins, support wiring in wigs, corset stays, non–precious-metal jewelry, and mascara (Steiger DA, unpublished data).

Although the chemical-shift dispersion of hydrogen in tissues is invaluable for spectroscopic investigations, chemical shift becomes a problem in evaluating images [21–23], especially those produced at very high fields where the ratio R_{CS} of chemical shift (CS) in frequency (Δf_{CS}) to bandwidth per pixel (Δf) is large. This ratio could, in turn, be reduced by increasing the read gradient but at the expense of S:N ratio. The effect is due to the fact that protons in water resonate at a different frequency than those in lipids. The chemical shift separation of fat and water protons is about 3.35 ppm [24], which corresponds to $\Delta f_{CS} = 71.4$ Hz at 0.5 T.

For values of R_{CS} less than unity, regions containing both water and fat will be unaffected for an ideal spin-echo sequence. If the timing of the 180° pulse is incorrect, the fat will gain a relative phase with respect to the water, and the intensity of the signal will change even though no shift in position occurs [25]. With or without these relative changes in phase, the two-component nature of the signal causes T1 and T2 to be inaccurately determined because of the now multiexponential nature of the signal. With new techniques that account for field inhomogeneities in the separation of water and fat [26], the separated components of T1 and T2 can be accurately found.

When R_{CS} is greater than unity, the fat is shifted by one or more pixels from its actual position with respect to the water. This may be a problem when a predominantly fat-containing area is shifted far enough to overlap a region of interest. This effect is significant in the orbit, where it may degrade what would otherwise be a high-resolution scan. It is also significant in the spine, where the superior and inferior margins of the vertebral bodies may show reduced or increased intensity, and in the kidneys (Fig. 14). Clinically, the shift is unimportant for brain imaging since the lipid (myelin) signal intensity from brain is negligible relative to that from water.

Similar intensity changes and distortions can occur from in vivo local field inhomogeneities because of tissue magnetic properties. These inhomogeneities are caused by changes in susceptibility between tissues (or air) in the body (for example, near the paranasal sinuses). These, as well as other field distortions, also cause local phase changes. For techniques that need phase information, such as water/fat separation, these phase changes can wreak havoc with the images. Techniques that account for such effects are then required [27].

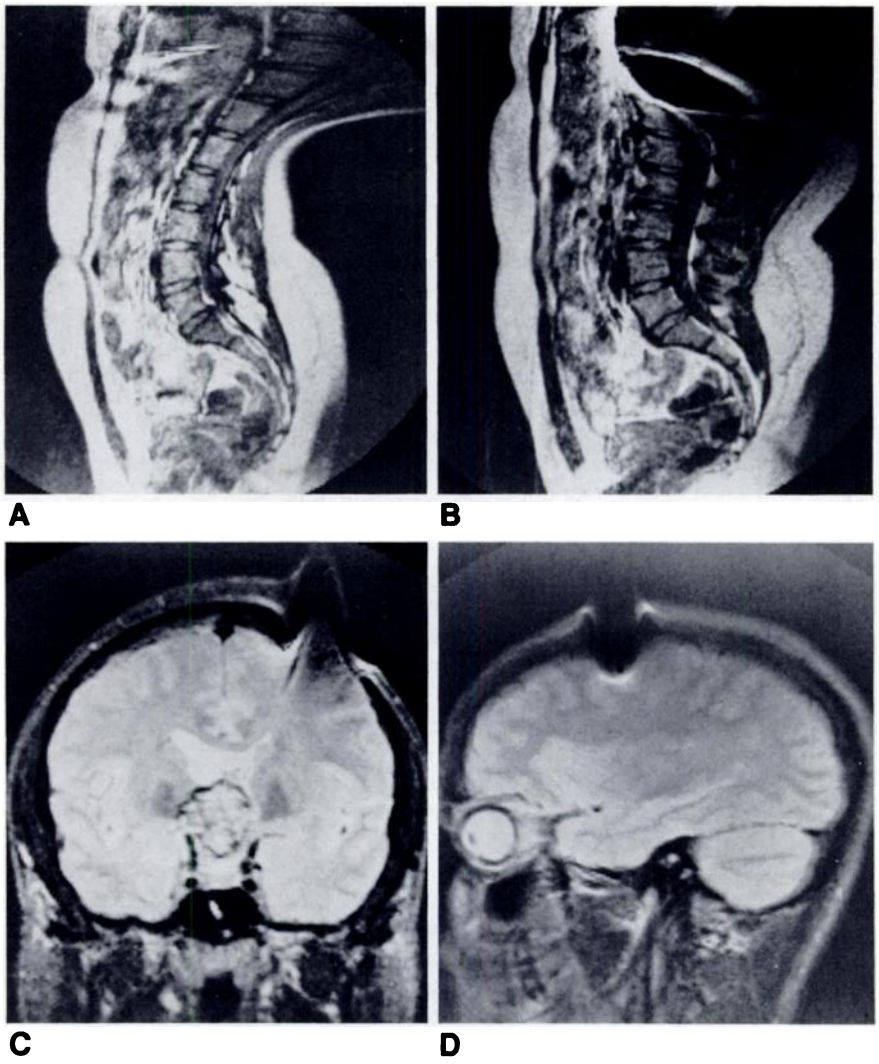

Fig. 13.—Bizarre ferromagnetic effects may occur, usually related to quantity, shape, and susceptibility of metal present. Note area of intensity extending well beyond anatomic boundaries of subject, in frequency-encoded direction.

***A* and *B*, Artifact caused by metal fasteners of a seven-hook bra. Note distortion is to left in *A* and to right in *B*. This is due to alternate-slice orientation of frequency-encoding gradient (see Fig. 10).**

***C* and *D*, Artifact due to shunt-tube reservoir. Note localized tearing and stretching of image (TR 2000, TE 40).**

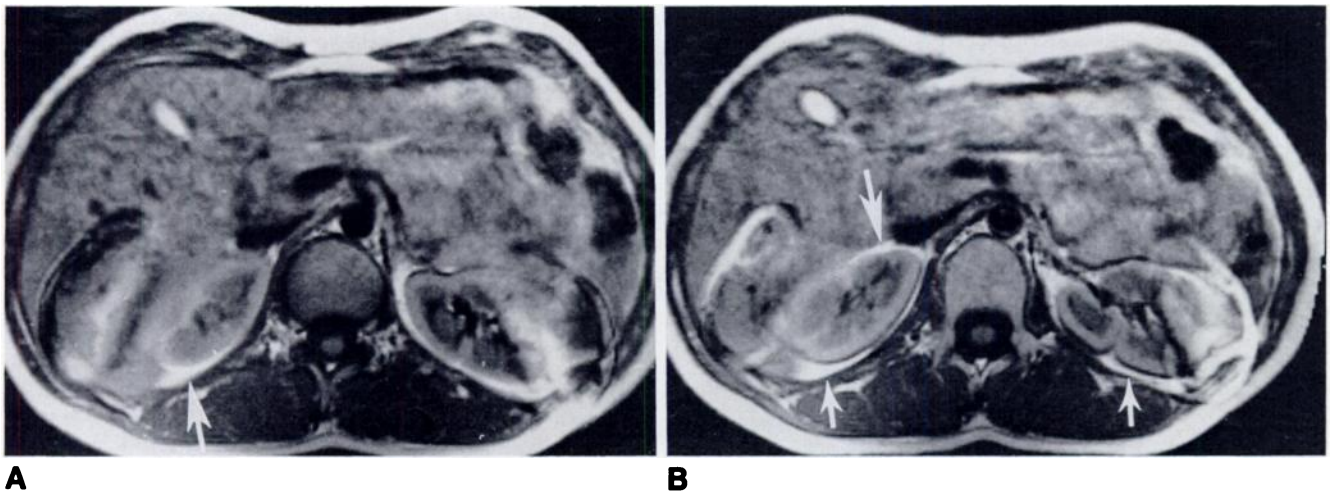

Fig. 14.—Chemical-shift artifact. *A* and *B*, Kidneys show area of intensity (*long arrows*) along inferior margin in *A* and superior edge in *B*. Also, in *B*, inferior margin has changed from intense to dark line (*short arrows*). Intensity change is caused by differential shift of protons in fat vs those in water, and occurs in frequency-encoded direction. In *A*, frequency-encoded direction is vertically upward, while in *B*, it is vertically downward. Changing direction of gradient is a useful method of confirming that changes observed are artifactual in nature. (TR 700, TE 40.)

Noise Artifacts

System-Related

Noise may be considered as any information in the signal that does not contribute to characterization of the biologic sample being imaged. Sources of white noise include random thermal variation in the sample and electronic noise from scanner hardware. Extraneous broadcast RF energy acts as another source of noise that affects a specific frequency. While scanner design optimization involves tradeoffs that maximize the S:N ratio, even under ideal circumstances the signal is generally only one or two orders of magnitude greater than the noise level.

Thermal (incoherent) noise produces diffuse increase in image mottle. The effects of thermal noise are diminished in surface-coil applications, where signal detection falls off rapidly as a function of depth, and the coil effectively does not see the thermal noise from more distant tissues [28].

Radiofrequency interference is due to detection of extraneous broadcast energy by the receiver coils of the scanner. Since the operating frequency of the scanner is directly related to magnet field strength, the frequency is essentially fixed around a narrow range (for example, 21.3 MHz for 0.5 T, or 64.0 MHz for 1.5 T), and any extraneous broadcast energy near this frequency may be detected. These sources include fluorescent lights (starter and ballast) and electric motors (especially direct current). Television and radio transmissions are also a problem, since 21.3 MHz is within the frequency assigned to amateur radio operators (21.0–21.5 MHz); 64.0 MHz falls within the frequency assigned to channel 3 (60–66 MHz); and 85.0 MHz lies within the FM radio band. Base-to-base and mobile communications are in the range 5–50 MHz. Similarly, 60 Hz noise in the electric power supply can also affect the image. The artifact produced is usually a linear band across the image (Fig. 15), apparent where the noise overwhelms the tissue signal. It is perpendicualr to the frequency-encoded direction, and its position is related to the difference in frequency between the center frequency of the scanner and the extraneous signal. This determines the distance to which the artifact is displaced from the center frequency (and thus from the center of the image).

Patient-Related

Systematic sources of noise are induced by nonideal circumstances in the scan. These include errors in establishing the correct phase relationship at each position due to nonlinear gradients, field inhomogeneities, motion, or flow. In particular, patient motion of any type degrades image quality because it produces data-phase errors. Phase information is used by the reconstruction algorithm in the process of voxel to pixel mapping. Motion-induced phase errors result in blurring, "ghosting," or mottled bands propagated in the phase-encoded direction. Even when the patient is externally quiescent, biologic activity associated with cardiac, respiratory, blood flow, and peristaltic motion continues. While the artifact produced by these activities may appear in the region of interest, it should not be considered as random white noise. It is in fact misregistered tissue information that cannot be properly positioned by current reconstruction algorithms. Future sequence and software developments [14, 15] will most likely correct phase errors so that physiologic motion will have a less detrimental effect on image quality.

For obvious reasons, motion produces a loss of resolution when it is significant with respect to the TR, as occurs, for example, when the patient turns, fidgets, or repositions a limb. This type of motion unsharpness is also seen with physiologic activities—the pancreas moves 2.0 cm on average in the craniocaudad direction during tidal respiration [29]. The magnitude of this excursion dwarfs the dimensions of the voxels commonly used in imaging and thus completely destroys the image. However, motion also induces phase

Fig. 15.—Radiofrequency artifact. Extraneous RF energy sources near scanner operational frequency produce linear band across image, perpendicular to frequency-encoded direction. Its exact position is determined by difference between center frequency of scanner and extraneous signal. (TR 600, TE 40.)

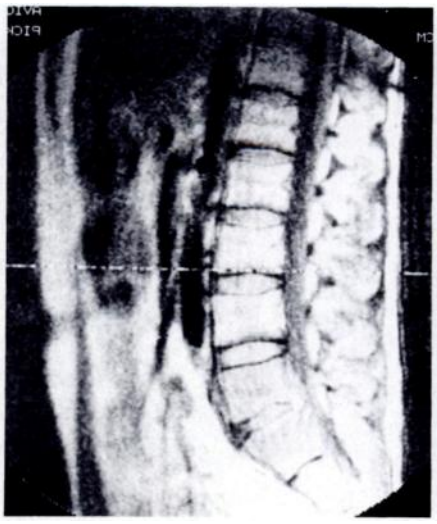

15

Fig. 16.—Swallowing artifact has produced horizontal band of noise along phase-encoded direction. Where it passes over vertebral body and spinal cord, there are local intensity and contrast changes, rendering these portions of scan suspect. If desired, artifact may be overcome by changing phase-encoded gradient to vertical direction, so that noise is propagated off regions of interest.

16

changes to which 2DFT is extremely sensitive (see later discussion). These phase changes lead to noise throughout the affected region along the phase-encoded direction.

Artifacts due to body-part motion, such as flow, blinking, swallowing, or chewing, are a form of coherent noise. Although often not important locally, they may affect a critical region of the image by producing a band of noise propagated across the field in the phase-encoded direction. This will cause areas of increased or diminished intensity in the region of interest, creating doubt as to the presence of abnormality and hence rendering the scan useless for diagnosis (Fig. 16). Flow artifacts from the internal carotid artery, carotid siphon, or jugular bulb are frequently encountered in scans of the head. They are much more evident in surface-coil applications because of the improved S:N ratio [7]. Depending on the image plane, the artifact may be redirected to noncritical areas of the image through proper selection of the phase-encoded direction. Phase-encoded flow artifacts may be seen in arteries, veins [10, 11], or any other fluid system, including the CSF [30, 31].

Chewing and talking produce mandibular, lingual, and laryngeal musculature motion that result in obvious image degradation, both locally and over the neck and cervical spine. Another problem occurs in imaging patients with oropharyngeal or laryngeal tumors, as well as lesions of the tongue and oropharynx, where secretions and saliva require frequent clearing and swallowing. This is also important with certain neurologic disorders involving the brainstem and lower cranial nerves.

Peristalsis may be a major source of artifact when the upper abdomen and pelvis are imaged (Fig. 17), especially with the longer scan sequences. Significant reduction is possible through use of glucagon to eliminate gastrointestinal tract peristalsis. Since the sensitive region of surface coils is limited, they can be positioned so as to receive signal from nonmoving tissue only [28, 32, 33], thus minimizing the noise.

Respiratory motion produces a form of coherent noise distributed across the image as a periodic artifact [14, 34]. In the head, the major contribution is from eye movement, while in the body the major contribution is from high-intensity areas in the subcutaneous and retroperitoneal fat. Throughout the body the pulsatile component of blood flow may also produce artifacts. These artifacts are produced in the phase-encoded direction, regardless of the direction of the motion causing them. The ghost images are partial copies of the original static structure, with interference effects producing areas of reinforcement or cancellation. In the case of respiratory artifacts, the ghost images become more widely separated with increasing respiratory rate or prolonged TR; increased respiratory amplitude produces only increased blurring of both the original and ghost images, but no positional change [8, 14, 28, 34, 35]. Multiple acquisitions can remove the worst of these artifacts if the product of the number of averages and TR is approximately equal to the respiratory period [14, 36].

The Gibbs phenomenon causes a ringing in the image (Fig. 18) due to data truncation [37]. This can resemble the periodic ghosting in the vicinity of edges as in the case of motion artifact.

Cardiac and respiratory motion produce sufficient pixel misregistration and phase shift to totally degrade the image, unless some form of gating or specialized data-collection method is used. Gating is a technique that essentially removes both motion problems (loss of resolution and phase-encoded noise). Although respiratory gating may extend scan times by factors of 2 to 4, significant image improvement results (Fig. 19). Methods using phase reordering to destroy the periodicity of the respiratory motion, such as centrally ordered phase encoding (COPE) and respiratory ordered phase encoding (ROPE) [14, 16, 17], remove only the phase-encoded smearing, without increasing the scan time. Figure 20 demonstrates the improvement achieved with COPE for dealing with respiratory motion. Without phase-encoded reordering, the noise

Fig. 17.—Peristalsis and respiratory artifacts. Wide band of artifact extends horizontally across anterior half of abdomen in phase-encoded direction. Blurring is caused by peristalsis, while curvilinear replication of subcutaneous fat (*arrows*) is caused by respiration.

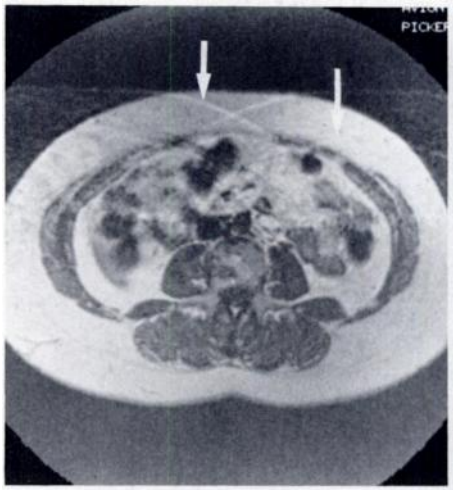

17

Fig. 18.—Ringing artifact due to data truncation. Note periodic nature of ringing. This should not be confused with motion artifact.

18

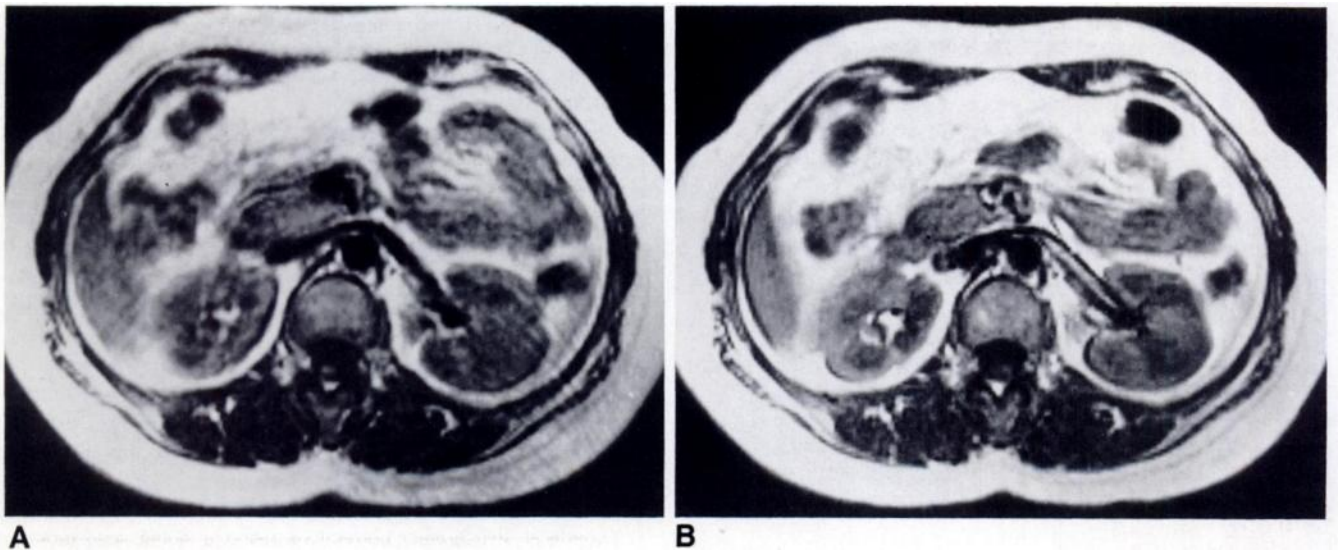

Fig. 19.—Respiratory gating. Transverse section through abdomen at level of head of pancreas and kidneys. Multislice scan (six slices), TR 500, TE 40.
***A*, Without gating, 4-min scan.**
***B*, With gating, 10-min scan.**

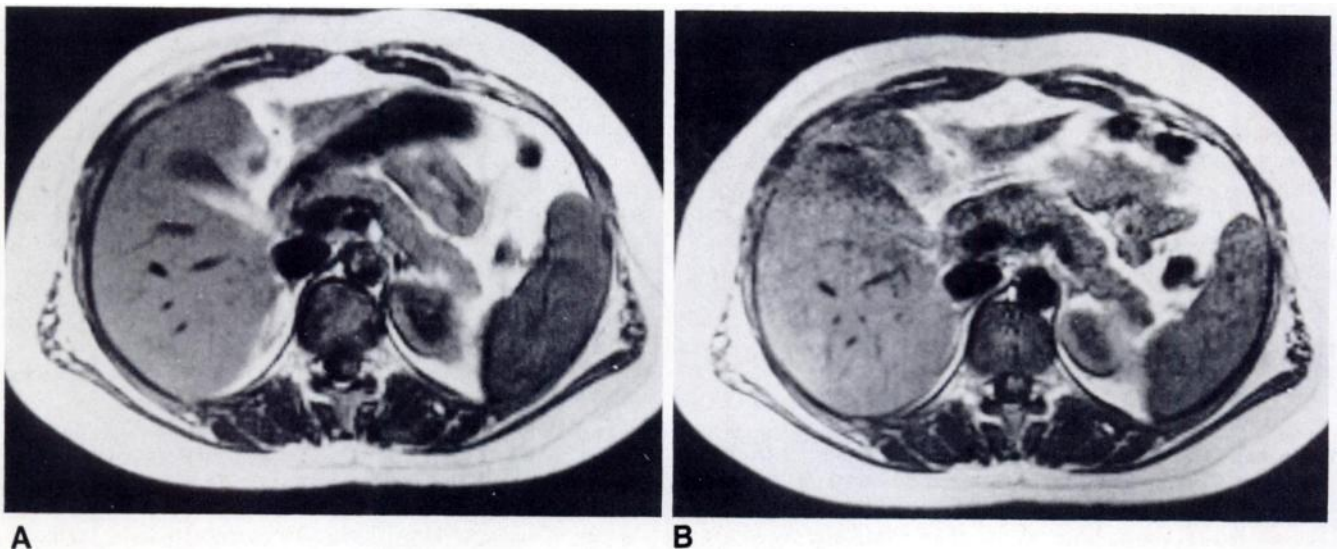

Fig. 20.—Respiratory artifact—improvement with COPE.
***A*, With respiratory gating, 10-min scan, TR 500, TE 40.**
***B*, Monitoring motion and collecting data with appropriate values of phase-encoded gradient according to COPE technique. Some small background noise artifact remains because actual movement itself has not been accounted for. Scan time was only 4 min.**

can also be reduced and redistributed by using the Hybrid fast-scan technique. In principle, both COPE and Hybrid could be combined to yield high-quality, short-time body images.

ACKNOWLEDGMENTS

We thank Michael A. Profeta, Eileen Strauss, Douglas Jarvis, and Jan Harrison for technical assistance; Laura Lewis for secretarial support; Michael Pettit and David Sabol for their photographic skills, and John Patrick, Leonard Weiss, and Ernest Wiesen for their contributions of time and information.

REFERENCES

1. Haacke EM, Clayton JR, Lampman DA, Linga NR. Artifacts in two-dimensional Fourier transform imaging (abstr). Program of the annual meeting of the Society of Magnetic Resonance in Medicine, New York, August **1984**:288–289
2. Yamanashi WS, Wheatley KK, Lester PD, Anderson DW. Technical artifacts in magnetic resonance imaging. *Physiol Chem Phys Med NMR* **1984**;16:237–250
3. Pusey E, Brown RKJ, Lufkin R, Solomon M, Hanafee W. Artifacts

in MR imaging: mechanisms and clinical significance (abstr). *Radiology* **1985**;157(P):296
4. Hastrup W, Porter BA, Olson DO, et al. Classification and investigation of artifacts in MR imaging (abstr). *Radiology* **1985**;157(P):397
5. Kulkarni MV, Patton JA, Wolfe O, et al. Techniques, pitfalls, and artifacts in MR imaging (abstr). *Radiology* **1985**;157(P):398
6. Haacke EM, Bellon EM. Artifacts produced by Fourier transform inversion techniques in magnetic resonance imaging. In: Stark DD, Bradley WG, eds. *Magnetic resonance imaging*. St. Louis: Mosby, in press
7. Glover GH, Hayes CE, Pelc NJ, et al. Comparison of linear and circular polarization for magnetic resonance imaging. *J Magnetic Resonance* **1985**;64:255–270
8. Ehman RL. MR imaging with surface coils. *Radiology* **1985**;157:549–550
9. Moran PR, Moran RA, Karstaedt N. Verification and evaluation of internal flow and motion. True magnetic resonance imaging by the phase gradient modulation method. *Radiology* **1985**; 154:433–441
10. Bradley WG, Waluch V, Lai K-S, Fernandez EJ, Spalter C. The appearance of rapidly flowing blood on magnetic resonance images. *AJR* **1984**;143:1167–1174
11. Bradley WG, Waluch V. Blood flow: magnetic resonance imaging. *Radiology* **1985**;154:443–450
12. Mansfield P, Pykett IL. Biological and medical imaging by NMR. *J Magnetic Resonance* **1978**;29:355–373
13. Haacke EM, Bearden FH, Clayton JR, Linga NR. Reduction of MR imaging time by the Hybrid fast-scan technique. *Radiology* **1986**;158:521–529
14. Haacke EM, Patrick JL. Reducing motion artifacts in two-dimensional Fourier transform imaging. *Magnetic resonance imaging* **1986**;4:359–376
15. Haacke EM. Application of a generalized transform to image reconstruction in MRI (abstr). Program of the annual meeting of the Society of Magnetic Resonance in Medicine, London, August **1985**:975–976
16. Bailes DR, Gilderdale DJ, Bydder GM, Collins AG, Firmin DN. Respiratory ordered phase encoding (ROPE): a method for reducing respiratory motion artefacts in MR imaging. *J Comput Assist Tomogr* **1985**;9:835–838
17. Haacke EM, Patrick JL, Bond CK, Blakely DM. Correction for motion artifacts based on a linear expansion model (abstr). Program of the annual meeting of the Society of Magnetic Resonance in Medicine, London, August **1985**:977
18. Finn EJ, Di Chiro G, Brooks RA, Sato S. Ferromagnetic materials in patients: detection before MR imaging. *Radiology* **1985**; 156:139–141
19. New PFJ, Rosen BR, Brady TJ, et al. Potential hazards and artifacts of ferromagnetic and nonferromagnetic surgical and dental materials and devices in nuclear magnetic resonance imaging. *Radiology* **1985**;147:139–148
20. Laakman RW, Kaufman B, Han JS, et al. MR imaging in patients with metallic implants. *Radiology* **1985**;157:711–714
21. Soila KP, Viamonte M, Starewicz PM. Chemical shift misregistration effect in magnetic resonance imaging. *Radiololgy* **1984**;153:819–820
22. Hricak H, Williams RD, Moon KL, et al. Nuclear magnetic resonance imaging of the kidney: renal masses. *Radiology* **1983**;147:765–772
23. Babcock EE, Brateman L, Weinreb JC, Horner SD, Nunnally RL. Edge artifacts in MR images: chemical shift effect. *J Comput Assist Tomogr* **1985**;9:252–257
24. Maudsley AA, Hilal SK. Field inhomogeneity correction and data processing for spectroscopic imaging. *Magnetic Resonance Med* **1985**;2:218–233
25. Dixon WT. Simple proton spectroscopic imaging. *Radiology* **1984**;153:189–194
26. Patrick JL, Haacke EM, Hahn JE. Evaluation of T1 and T2 from water and fat separated images (abstr). *Radiology* **1985**; 157(P):220
27. Patrick JL, Haacke EM, Hahn JE. Water/fat separation and chemical shift artifact corrections using a single scan (abstr). Program of the annual meeting of the Society of Magnetic Resonance in Medicine, London, August **1985**:174–175
28. White EM, Edelman RR, Stark DD, et al. Surface coil MR imaging of abdominal viscera. Part II. The adrenal glands. *Radiology* **1985**;157:431–436
29. Suramo I, Paivansalo M, Myllyla V. Cranio-caudal movements of the liver, pancreas and kidneys in respiration. *Acta Radiol [Diagn]* (Stockh) **1984**;25:129–131
30. Bradley WG, Kortman KE, Burgoyne B. The variable MR intensity of ventricular CSF: effect of flow (abstr). Program of the annual meeting of the Society of Magnetic Resonance in Medicine, London, August **1985**:319–320
31. Sherman JL, Citrin CM. Magnetic resonance demonstration of normal CSF flow. *AJNR* **1986**;7:3–6
32. Edelmann RR, McFarland E, Stark DD, et al. Surface coil MR imaging of abdominal viscera. Part I. Theory, technique, and initial results. *Radiology* **1985**;157:425–430
33. Simeone JF, Edelman RR, Stark DD, et al. Surface coil MR imaging of abdominal viscera. Part III. The pancreas. *Radiology* **1985**;157:437–441
34. Wood ML, Henkelman RM. MR imaging artifacts from periodic motion. *Med Phys* **1985**;12:143–151
35. Schultz CL, Alfidi RJ, Nelson AD, Kopiwoda SY, Clampitt ME. The effect of motion on two-dimensional Fourier transformation magnetic resonance images. *Radiology* **1984**;152:117–121
36. Haacke EM, Lenz GW, Nelson AD. Pseudo-gating: elimination of periodic motion artifacts in magnetic resonance imaging without gating. *Magnetic Resonance Med*, in press
37. Wood ML, Henkelman RM. Truncation artifacts in magnetic resonance imaging. *Magnetic Resonance Med* **1985**;2:517–526